



Università degli Studi Mediterranea di Reggio Calabria
Archivio Istituzionale dei prodotti della ricerca

A Visual Programming Tool for Assessing Out-of-Plane Collapse in Masonry Walls

This is the peer reviewed version of the following article:

Original

A Visual Programming Tool for Assessing Out-of-Plane Collapse in Masonry Walls / Pisano, A. A.; Lasorella, M.; Percolla, G.; Fuschi, P.. - 1291:(2026), pp. 41-58. [10.1007/978-3-032-11926-1_3]

Availability:

This version is available at: <https://hdl.handle.net/20.500.12318/163866> since: 2026-01-18T10:12:53Z

Published

DOI: http://doi.org/10.1007/978-3-032-11926-1_3

The final published version is available online at: <https://link.springer.com/chapter/10.1007/978-3-032->

Terms of use:

The terms and conditions for the reuse of this version of the manuscript are specified in the publishing policy. For all terms of use and more information see the publisher's website

Publisher copyright

This item was downloaded from IRIS Università Mediterranea di Reggio Calabria (<https://iris.unirc.it/>) When citing, please refer to the published version.

(Article begins on next page)

07 May 2026



A Visual Programming Tool for Assessing Out-of-Plane Collapse in Masonry Walls

Aurora Angela Pisano^(✉), Mariaceleste Lasorella, Giulia Percolla, and Paolo Fuschi

Department of Architecture and Design – dAeD, University Mediterranea of Reggio Calabria,
Reggio Calabria, Italy

{aurora.pisano, mceleste.lasorella, giulia.percolla,
paolo.fuschi}@unirc.it

Abstract. The present paper focuses on the assessment and preservation of the structural safety of traditional masonry constructions by predicting their most probable collapse mechanism. The aim is to propose an efficient numerical approach for evaluating collapse in historical masonry structures, based on kinematic limit analysis applied to common local failure mechanisms and implemented through a visual scripting computational tool. The method integrates linear programming optimization within a CAD environment, utilizing an interactive Python component to compute the collapse load multiplier. The structural model is based on rigid blocks, following Heyman's assumptions. The effectiveness of the visual scripting framework is validated through the systematic evaluation of out-of-plane collapse mechanisms of masonry walls, demonstrating its potential for rapid and accurate structural safety assessments.

Keywords: visual scripting · optimization algorithm · masonry macro-blocks · kinematic limit analysis

1 Introduction

The preservation of the Italian cultural heritage is a crucial and widely discussed topic, addressed from various perspectives. Among these, particular attention is given to the structural safety of historic buildings, the majority of which are constructed with masonry. The structural integrity of these masonry constructions is influenced by a variety of factors, which must be carefully considered to ensure their long-term safety. Some of these factors are related to aspects inherent to the construction, such as the properties of materials used (e.g., compressive strength, porosity, presence of defects) and the construction techniques employed (e.g., mortar type, masonry quality, connections between elements). On the other hand, further factors depend on external conditions and involve forces acting upon the building. These include applied loads, e.g., permanent weights, variable loads, seismic forces, but also non mechanical actions like the ones exerted by sunlight, humidity, climatic actions and climate change in general. Such factors can lead to degradation and reduced durability of the masonry. Moreover, the interaction between internal and external factors determines the actual load-bearing capacity and vulnerability of the structure (Giuffrè, 1996) (Szabó et al., 2023).

© The Author(s) 2026

C. Nava et al. (Eds.): *Climatic and Structural Safety in Multi-Hazard Regime of Cultural and Natural Heritage*, GREEN, pp. 41–58, 2026.

https://doi.org/10.1007/978-3-032-11926-1_3

The strong interest in the preservation of the architectural heritage and the complexity of the problem led to the development of various methods to assess the structural safety of masonry buildings. The choice of the appropriate method requires evaluating its specific advantages and limitations in relation to the structural problem at hand. A fundamental classification of masonry assessment approaches is based on the type of analysis method used to study the mechanical behavior of masonry and on how the masonry material is modeled within the method itself. A detailed overview is provided in the review by D'altri et al. (2020). In particular, analysis methods are generally categorized as: *nonlinear incremental approaches* and *direct or limit analysis ones*. While material modeling approaches include: *continuum mechanics-based models* and *rigid-block models* representing masonry as assemblies of discrete blocks.

The first category of approaches comprises nonlinear incremental methods primarily aimed at numerically simulating the full mechanical response of masonry structures, incorporating assumptions across different material scales and accounting for damage and interface effects. Recent studies employ finite element methods (FEM), often coupled with probabilistic approaches to address uncertainties in parameters used in FE analyses (Mazzeo et al., 2024). For instance, Galassi and Zampieri (2023) present an automated nonlinear incremental procedure to predict failure and collapse mechanisms in masonry arches, evaluating internal forces at block joints under equilibrium and continuity constraints. Similarly, Portioli and Lourenço (2024) propose a rigid-block model with elastoplastic softening interfaces for nonlinear static analysis, validated experimentally and numerically, focusing on material softening and failure mechanisms.

Nonlinear incremental methods provide insight, for example, into the seismic behavior of masonry, but face practical constraints: accurately modeling the heterogeneity and anisotropy of masonry requires detailed mechanical, material, and geometric parameters, making simulations computationally demanding; moreover, their strong sensitivity to input uncertainties can lead to wide variability in the predicted responses, limiting their use in real-world applications. All these factors necessitate careful consideration for selecting an appropriate technique for the assessment of masonry structures (Kumar et al., 2022).

On the other hand, limit analysis methods, despite their own limitations, provides a robust efficient framework alternative to nonlinear approaches. Indeed, they result particularly attractive when detailed material modeling and simulation are not feasible, offering key benefits in speed, accuracy for specific failure modes, and adaptability to various geometries. Limit analysis is, in fact, effective in predicting collapse loads, without modeling the full failure process. It is essentially based on equilibrium conditions which enhances its applicability in both seismic and non-seismic scenarios. Numerous local collapse phenomena have been studied and classified in this context (Milano et al., 2009), providing case studies to identify potential triggers of structural failure. The Italian regulatory framework (MIT, 2019) explicitly permits the application of limit analysis when assessing local collapse mechanisms. Consequently, numerous methods for masonry safety assessment are grounded on limit analysis theory, utilizing both static and kinematic approaches. These methods stem from the recognition that structural collapse often initiates from the localized instability of macro-elements.

Moreover, the numerical limit analysis methods, which frequently incorporate optimization algorithms, offer another significant advantage that is the capability of determining collapse loads and failure mechanisms even in complex geometries. Notably, in Baggio and Trovalusci (2000) the authors have explored nonlinear programming with friction for modeling masonry as rigid blocks, considering interface dilatancy. This allows for a more complete understanding of structural behavior under stress, especially for systems with irregular shapes or complex boundary conditions. Another advantage of limit analysis is its flexibility in modeling frictional interfaces, which significantly influence collapse mechanisms. Methods proposed by Ferris and Tin-Loi (2001) utilize constrained optimization to account for non-associative friction and tension-free contact, while in (Gilbert et al., 2006) a linear programming approach is introduced to model non-associative frictional joints. In (Gilbert, 2007) an efficient kinematic-based numerical method is also developed for bearing capacity assessment, further emphasizing the versatility of limit analysis in a wide range of scenarios. Nodargi et al. (2019) implemented a variational fixed-point algorithm for limit analysis of dry-masonry block structures considering frictional interfaces. Kinematic limit analysis approaches have instead been applied by Casapulla et al. (2023) for seismic vulnerability of masonry walls with or without grouted anchors. Although efficient, many applications of limit analysis are still restricted to idealized geometries and oversimplified collapse scenarios, which reduces their applicability to complex real-world masonry structures.

In the authors' opinion, in recent years, limit analysis has gained more attraction in professional practice through its integration within visual scripting environments, which enables efficient, interactive safety assessments of masonry structures. Pioneering work by (Block, 2009) introduced Thrust Network Analysis in CAD software, further improved in (Rippmann et al., 2012). In (Stockdale & Milani, 2019) a similar technique is applied in AutoCAD for arch safety evaluations. More recently, Funari et al. (2021) developed a Grasshopper-based tool in Rhinoceros that allows interactive and parametric exploration of collapse mechanisms via genetic algorithms. Mousavian et al. (2021) implemented a Grasshopper plugin for out-of-plane collapse in multi-storey walls, using a macro-block limit analysis that accounts for geometric and construction parameters. These recent developments demonstrate that embedding limit analysis in visual scripting environments delivers rapid, user-friendly, and computationally efficient workflows for both design and heritage conservation.

While previous studies have already demonstrated the potential of integrating limit analysis with visual programming, the present work aims to further develop this potential by refining the approach and emphasizing its effectiveness and broader applicability. Therefore, this study contributes to the current trend of coupling limit analysis with CAD tools by employing Grasshopper for safety evaluations of masonry walls. The promoted approach merges limit analysis, carried on masonry walls treated as a system of rigid macro-blocks, with a linear-programming optimization to identify collapse mechanisms and determine the corresponding load multiplier in real time. This approach, as already outlined, is particularly advantageous when detailed material behavior modeling is impractical due to the inherent complexity and variability of masonry

materials. Through parametric inputs, users can instantly estimate how material, geometric, and loading variations influence structural behavior and test restoration or emergency intervention strategies. In line with recent advances in structural engineering, this study contributes to bridging the gap between theoretical research and practical heritage conservation tools. The paper is organized into five sections: after this introduction, Sect. 2 covers the theoretical background; Sect. 3 examines eight benchmark collapse mechanisms; Sect. 4 details the Grasshopper implementation; Sect. 5 offers concluding observations and future directions.

2 Theoretical Background

Limit analysis is here applied in its kinematic formulation also assuming that a masonry wall is modeled as an assembly of rigid, interlocked blocks under Heyman's hypotheses of zero tensile strength, infinite compressive strength and absence of sliding between blocks (Heyman, 1966). These assumptions apply to good-quality masonry with pre-existing interface cracks between visible, or recognizable, macro-elements.

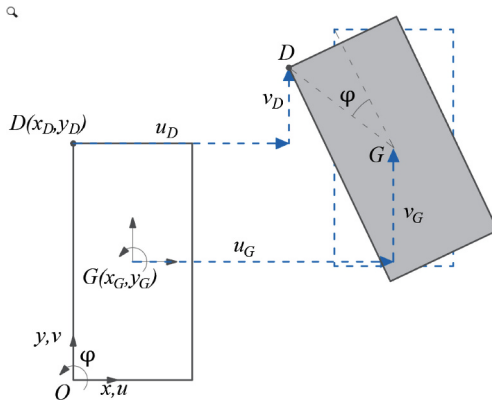


Fig. 1. Kinematic parameters related to the centroidal transverse section of the macro-element.

The procedure determines the collapse load multiplier, α , and the associated out-of-plane failure mechanism for each macro-element in the 2D plane of its centroidal transverse section (Fig. 1).

Referring to a global coordinate system (O, x, y) , the displacement $\mathbf{u}_D = [u_D, v_D]^T$ of a point $D(x_D, y_D)$ on a macro-element can be written in terms of the horizontal and vertical displacements u_G and v_G of the macro-element centroid G , together with its rotation φ around G . The latter three parameters are assembled into the vector \mathbf{d} :

$$\mathbf{d} = [u_G, v_G, \varphi]^T. \quad (1)$$

Displacements are taken positive when aligned with the global axes, as shown in Fig. 1. Moreover, the components u_D and v_D of the displacement vector can be defined

by the kinematic matrix \mathbf{S} defined as:

$$\mathbf{S} = \begin{bmatrix} 1 & 0 & -(y_D - y_G) \\ 0 & 1 & (x_D - x_G) \end{bmatrix}. \quad (2)$$

The displacement vector \mathbf{u}_D can therefore be written as:

$$\mathbf{u}_D = \mathbf{S}\mathbf{d} \quad (3)$$

The kinematic description above enables characterization of the collapse mechanism via limit analysis. Specifically, the kinematic formulation leads to an optimization problem that minimizes the virtual work required to induce collapse. The application of the principle of virtual work yields the equilibrium condition equating the work of stabilizing dead loads, all collected in the vector \mathbf{P}_d , with that of destabilizing live loads, all collected in the vector \mathbf{P}_l ; namely:

$$\mathbf{U}_d^T \mathbf{P}_d = \alpha \mathbf{U}_l^T \mathbf{P}_l \quad (4)$$

where \mathbf{U}_d and \mathbf{U}_l denote the displacement vectors of the application points of \mathbf{P}_d and \mathbf{P}_l , respectively and α is the live loads multiplier. When the crack pattern is specified a priori, the collapse multiplier α can be obtained directly from the virtual-work balance (Eq. 4), as for the simple overturning mechanism of a masonry macro-element, see e.g. (Cifani, et al., 2006). Conversely, if the crack geometry is not known in advance, this explicit expression no longer holds and α must be determined by solving an optimization problem that searches for the most critical collapse configuration, as in the approaches proposed by (Ferris & Tin-Loi, 2001), (Gilbert, 2007) and (Nodargi et al., 2019).

Two collapse scenarios are considered for a masonry wall macro-element with fixed hinge A and roller B (Fig. 2(a,b)), reflecting crack patterns observed in situ. In the first scenario (Fig. 2(a)), the macro-element rotates about hinge A. In the second scenario (Fig. 2(b)), an internal hinge C appears at an undetermined height, dividing the macro-element into two sub-elements. This vertical bending mechanism often occurs in historic façade walls and the location of hinge C enters an optimization algorithm to identify the most critical collapse configuration. To formulate the optimization problem, a parameter $\mu > 1$ is introduced that defines the ratio between the unknown block heights h_1 and h_2 , thereby fixing the internal hinge location. Specifically, for $\mu > 1$ the heights satisfy:

$$h_2 = \frac{h}{\mu}; \quad h_1 = \frac{\mu - 1}{\mu}; \quad \text{with } \mu > 1 \quad (5)$$

The optimization seeks the multiplier α from balance Eq. (4), subject to the constraint on μ , namely:

$$\min \alpha = \min_{\mu} \left[\frac{\mathbf{U}_d^T \mathbf{P}_d}{\mathbf{U}_l^T \mathbf{P}_l} \right] \quad \text{s.t. } \mu > 1. \quad (6)$$

The optimization problem defined in Eq. (6) seeks the minimum collapse multiplier α under the constraint $\mu > 1$. This strict inequality guarantees that the internal hinge lies within the macro-element rather than at its extremity. The resulting linear-programming formulation is hereafter solved in Python using the *linprog* function.

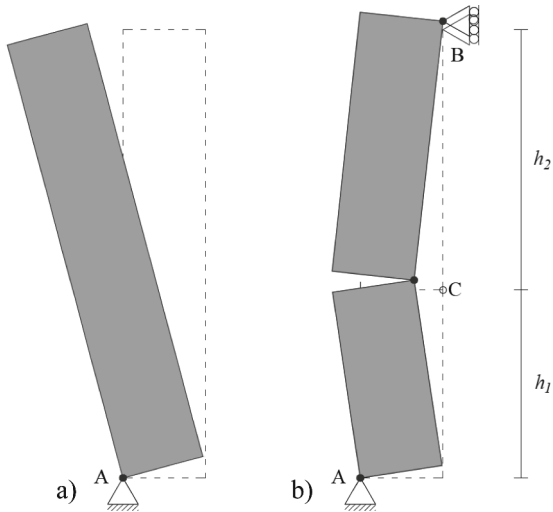


Fig. 2. Schematic representation of a masonry macro-element collapse mechanism: (a) simple overturning of a single macro-element around the external hinge A; (b) vertical bending of two interconnected macro-elements rotating around the internal hinge C, whose position is unknown.

3 Benchmark Collapse Mechanisms

Eight out-of-plane collapse mechanisms have been implemented, all falling under the two general categories introduced in the previous Sect. 2. Such mechanisms arise when external actions, most notably seismic forces, overcome the equilibrium of an entire wall or large wall segments. Their activation depends on factors governing out-of-plane response, including the quality of orthogonal wall connections, wall-to-wall interactions, roof configuration, opening layout, loads from upper stories, and even the building's position within the urban fabric. The considered mechanisms can be divided into *overturning mechanisms* and *bending mechanisms*. Overturning mechanisms may be *simple*, involving rotation of a single wall segment, or *composed*, if adjacent orthogonal wall portions are also dragged into motion; each mechanism can occur at one story or span multiple stories. Bending mechanisms are categorized by the orientation of the bending plane, *vertical* or *horizontal* and they too may affect a single level or multiple levels of the structure.

Tables 1, 2 and 3 schematically illustrate the eight out-of-plane collapse mechanisms addressed here, based on the classification of Milano et al. (2009), precisely: simple overturning of a single-story wall; simple overturning of a multi-story wall; composed overturning of a single-story wall; composed overturning of a multi-story wall; composed overturning of a corner wall; vertical bending of a single-story wall; vertical bending of a multi-story wall; and horizontal bending of a single-story wall. Each mechanism is represented in detail on the left column of Tables 1, 2 and 3, while in the right column the analytical expression of the corresponding collapse load multiplier is reported.

A simple description of each benchmark collapse mechanism is given next:

Simple Overturning of a Single-Story Wall

This mechanism affects a full single-story wall or a wide segment of it when out-of-plane forces cause it to move independently from adjacent sidewalls, as shown in Table 1(a). The wall rotates rigidly about a horizontal cylindrical hinge at its base, which spans the entire width of the macro-element. This simple overturning usually occurs at the topmost story or just below the roof. The analysis considers the centroidal transverse section of the wall, using the geometry, boundary conditions and loading depicted in Table 1(a). Specifically, W is the self-weight of the wall, F_v denotes the vertical thrust from arches or vaults, and P_s represents the floor or roof weight acting on the wall. Horizontal inertia forces arise by multiplying each of these vertical actions by the collapse multiplier α . The loads P_h and F_h account respectively for the static load from any head cover at the top of the macro-element and the horizontal thrust component of arches or vaults, while T represents the action of tie rods.

Simple Overturning of a Multi-Story Wall

This mechanism concerns a multi-story façade or large segments of it that, under out-of-plane forces applied at various levels, can detach from adjacent sidewalls (Table 1(b)). The wall undergoes rigid rotation about a known horizontal cylindrical hinge at its base, which spans the entire width of the macro-element. By analogy with the single-story case and using the same notation, the simple overturning of this multi-story macro-element is analyzed via its centroidal transverse section, with geometry, boundary conditions, and loads as shown in Table 1(b).

Composed Overturning of a Single-Story Wall

This mechanism concerns a single-story façade together with adjoining sidewall segments modeled as diagonal wedges (Table 1(c)). Under out-of-plane loading, the entire rigid macro-element rotates about a known horizontal cylindrical hinge at its base spanning its full width. The 2D analysis is carried out on the symmetry plane of this assembly, where the façade's centroidal section and the projected diagonal wedges, along with all applied forces, are treated as acting within that symmetry plane (Table 1(c)). This projection preserves the equilibrium of moments about the hinge.

Composed Overturning of a Multistory Wall

This mechanism addresses a multi-story façade and its adjoining sidewall segments, which extend across multiple levels and are idealized as paired diagonal wedges (Table 2(a)). Under out-of-plane loading, the entire rigid macro-element rotates about a fixed horizontal cylindrical hinge at its base spanning its full width. The analysis is conducted in 2D on the symmetry plane of this assembly, applying the same simplifying assumptions as before (Table 2(a)).

Composed Overturning of a Corner Wall

The corner-wedge mechanism is generated by two diagonal cracks along orthogonal walls, causing a rigid block to detach and rotate about a fixed hinge at the macro-element's base, as shown in Table 2(b). Typically observed in isolated buildings, this failure concentrates thrust at wall intersections. Assuming a 45° rotation plane (Table 2(b)),

the analysis projects all loads, including the ridge-beam load P and the vertical and horizontal components P_{v1} , P_{v2} , and P_{h1} and P_{h2} , onto this plane (Table 2(b)).

Vertical Bending of a Single-Story Wall

The mechanism involves two rigid blocks in which the original macro-element divides. The mechanism is the one typical of a façade wall rotating out of plane about a horizontal cylindrical hinge that forms between successive levels, as shown in Table 3(a). Vertical cracks at the junctions with adjacent sidewalls define the detached wedge, which is typically restrained by tie rods or beams at the story's top and bottom. The 2D model on this symmetrical plane (Table 3(a)) includes a vertical load N applied at the macro-element's top. External hinges A and B are fixed a priori, while the intermediate hinge C height emerges from an optimization involving the blocks' weights W_1 , W_2 and heights h_1 , h_2 via the parameter μ .

Vertical Bending of a Multi-Story Wall

This mechanism mirrors the previous case but occurs in a multi-story façade wall—i.e., a wall spanning more than two levels where intermediate connections are ineffective—and involves out-of-plane rotation of the above mentioned two rigid blocks about a horizontal cylindrical hinge (Table 3(b)). The same considerations apply, and the 2D mechanical model is shown in Table 3(b).

Horizontal Bending of a Single-Story Wall

The mechanism ejects the top portion of a façade wall under out-of-plane loading, detaching wedge- or trapezoidal-shaped blocks via oblique vertical cylindrical hinges (Table 3(c)). This collapse mode typically affects the uppermost story when strong sidewall connections prevent overall overturning, but weak roof connections permit horizontal bending of the wall. The detached segment rotates as two rigid blocks, once again formed by the division of the original macro-element, about fixed hinges A and B at its base and an internal hinge C at an undetermined position (Table 3(c)), analyzed in the horizontal rotation plane of the block edges. The collapse multiplier is defined by balancing all applied loads—where H is the reaction from a bracing wall or tie rod, and P_{hi} and P_{vi} are the horizontal and vertical components of roof loads—and the hinge coordinates L_1 , L_2 are functions of the optimization parameter μ , analogous to h_1 and h_2 in the vertical-bending case.

Table 1. Collapse mechanisms of overturning-type.

Overturning mechanism	
<p>The diagram shows a vertical wall of height h and base width s. A pivot point A is at the bottom left. A horizontal force P_h and a vertical force P_s are applied at the top. A horizontal force T is applied at the top right. Internal forces F_v and F_h are shown at a height h_v. The weight W and center of gravity G are also indicated. Distances d and d_v are marked from the pivot to the top force application points. The horizontal distance from the pivot to the center of gravity is y_G.</p>	$\alpha = \frac{W \cdot \frac{s}{2} + F_v \cdot d_v + P_s \cdot d + T \cdot h - F_h \cdot h_v - P_h \cdot h}{W \cdot y_G + F_v \cdot h_v + P_s \cdot h}$
a) Simple overturning of a single-story wall	
<p>The diagram shows a two-story wall with total height h_{tot}. The top story has height h_2 and width s_2. The bottom story has height h_1 and width s_1. Forces P_{s1}, P_{h1}, T_1 are applied at the top of the first story, and P_{s2}, P_{h2}, T_2 are applied at the top of the second story. Internal forces F_{v1}, F_{h1}, W_1, G_1 and F_{v2}, F_{h2}, W_2, G_2 are shown. Distances d_{v1}, d_{v2} and d_{h1}, d_{h2} are marked. The horizontal distance from the pivot to the center of gravity of the first story is y_{G1}, and for the second story it is y_{G2}.</p>	$\alpha = \frac{[\sum_i W_i \cdot \frac{s_i}{2} + \sum_i F_{vi} \cdot d_{vi} + \sum_i P_{si} \cdot d_i + \sum_i T_i \cdot h_i - \sum_i F_{hi} \cdot h_{vi} - P_h \cdot h_{tot}]}{[\sum_i W_i \cdot y_{Gi} + \sum_i F_{vi} \cdot h_{vi} + \sum_i P_{si} \cdot h_i]}$
b) Simple overturning of a multi-story wall	
<p>The diagram shows a vertical wall of height h and base width s. A pivot point A is at the bottom left. A horizontal force P_h and a vertical force P_s are applied at the top. A horizontal force T is applied at the top right. Internal forces F_v and F_h are shown at a height h_v. The weight W and center of gravity G are also indicated. Distances d and d_v are marked from the pivot to the top force application points. The horizontal distance from the pivot to the center of gravity is y_G. An additional weight W_O and center of gravity G_O are shown at a horizontal distance x_{GO} from the pivot.</p>	$\alpha = \frac{[W \cdot \frac{s}{2} + F_v \cdot d_v + W_O \cdot x_{GO} + P_s \cdot d + P_{s0} \cdot d_o + T \cdot h - F_h \cdot h_v - P_h \cdot h]}{[W \cdot y_G + W_O \cdot y_{GO} + F_v \cdot h_v + P_s \cdot h + P_{s0} \cdot h]}$
c) Composed overturning of a single-story wall	

Table 2. Collapse mechanisms of overturning-type.

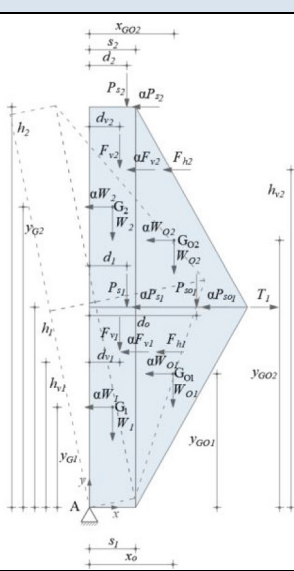
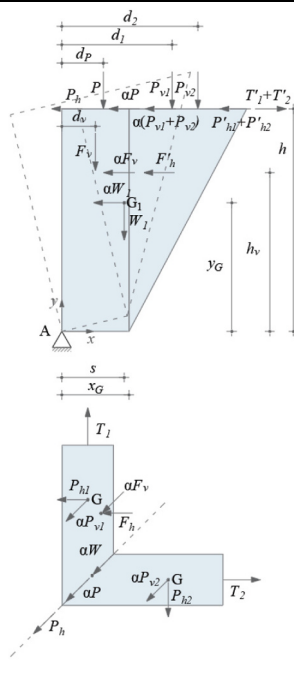
Overturning mechanism	
	$\alpha = \frac{num}{\sum_i W_i y_{GOi} + \sum_i W_{oi} y_{GOi} + \sum_i F_{vi} h_{vi} + \sum_i P_{si} h_i + \sum_i P_{soi} h_i}$ $num = \sum_i W_i \frac{s_i}{2} + \sum_i F_{vi} d_{vi} + \sum_i W_{oi} x_{GOi}$ $+ \sum_i P_{si} d_i + \sum_i P_{soi} d_{oi} + \sum_i T_i h_i - \sum_i F_{hi} h_{vi}$
d) Composed overturning of a multistory wall	
	$\alpha = \frac{num}{W y_G + F_v h_v + (P + P_{v1} + P_{v2}) h}$ $num = W x_G + F_v d_v + P d_p + P_{v1} d_1 + P_{v2} d_2$ $+ (T_1 + T_2) h - F'_h h_v - (P_h + P'_{h1} + P'_{h2}) h$
e) Composed overturning of a corner wall	

Table 3. Collapse mechanisms of bending-type.

Bending mechanism	
	$\alpha = 2 \frac{(\mu - 1)(N d + P_s a + F_v d_v - F_h h_v) + s(W + N + P_s + F_v)}{(\mu - 1)(W h / \mu + 2 F_v h_v)}$ $h_1 = \frac{\mu - 1}{\mu} h \quad h_2 = \frac{h}{\mu} \quad W_2 = \frac{W}{\mu} \quad W_1 = \frac{\mu - 1}{\mu} W$
f) Vertical bending of a single-story wall	
	$\alpha = \frac{num}{W_1 y_{G1} + F_{v1} h_{v1} + P_{s1} h_{p1} + (W_2 y_{G2} + F_{v2} h_{v2}) (h_1 / h_2)}$ $num = W_1 x_{G1} + W_2 \left(s_2 + x_{G2} \frac{h_1}{h_2} \right) + F_{v1} d_{v1} + F_{v2} s_2$ $+ F_{v2} \frac{h_1}{h_2} d_{v2} + P_{s1} a_1 + P_{s2} \left(s_2 + a_2 \frac{h_1}{h_2} \right)$ $+ N \left(s_2 + d \frac{h_1}{h_2} \right) + T_1 h_{p1} - F_{h1} h_{v1} - F_{h2} h_v \frac{h_1}{h_2}$ $h_1 = \frac{\mu - 1}{\mu} h, h_2 = \frac{h}{\mu}, W_2 = \frac{W}{\mu}, W_1 = \frac{\mu - 1}{\mu} W$
g) Vertical bending of a multi-story wall	
	$\alpha = \frac{H s \left(1 + \frac{L_1}{L_2} \right) - \sum_i P_{hi1} d_{i1} - \sum_i P_{hi2} \frac{L_1}{L_2} d_{i2}}{W_1 x_{G1} + W_2 \frac{L_1}{L_2} x_{G2} + \sum_i P_{vi1} d_{i1} + \sum_i P_{vi2} \frac{L_1}{L_2} d_{i2}}$ $L_1 = \frac{\mu - 1}{\mu} L, L_2 = \frac{L}{\mu}, W_2 = \frac{W}{\mu}, W_1 = \frac{\mu - 1}{\mu} W$
h) Horizontal bending of a single-story wall	

4 Visual Programming Framework for Limit Analysis

The limit analysis optimization is implemented within Grasshopper, the visual scripting environment of Rhinoceros, enabling direct input of CAD geometries for masonry walls. This delivers an interactive workflow in which the kinematic limit analysis automatically identifies the most probable collapse mechanism and computes the corresponding load multiplier in real time. Figure 3 outlines the workflow as a series of Grasshopper components, organized into colored sections. The process is illustrated using one of the benchmark cases, addressed previously, namely the vertical bending mechanism in a two-story masonry wall.

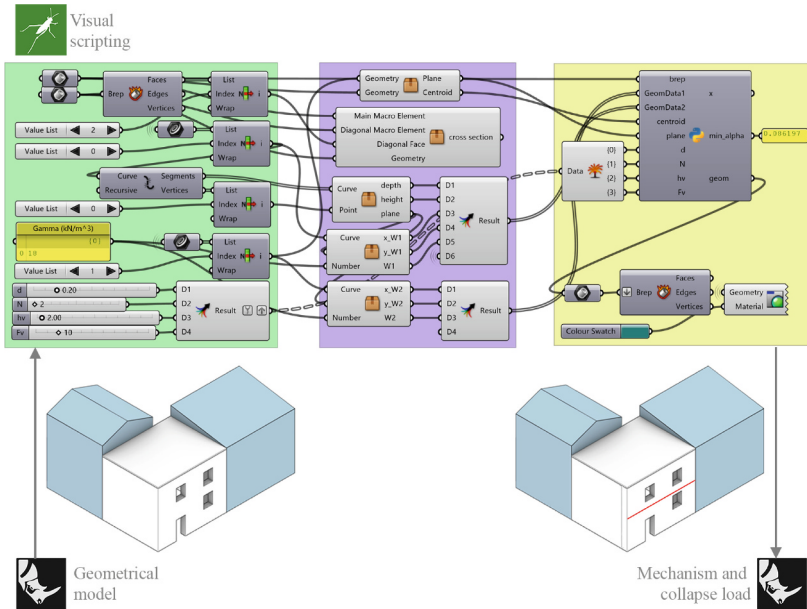


Fig. 3. Sketch of the workflow of the visual scripting approach for performing limit analysis on a double-story masonry façade with a vertical bending mechanism.

The process begins by defining the geometry of the two macro-elements and importing the CAD model into Grasshopper. The user then selects the relevant wall cross-section, i.e., the plane of potential mechanism rotations and specifies boundary conditions, applied loads, and material properties as shown in the green section (on the left) of Fig. 3. In the lilac section (center) the script automatically detects and extracts all necessary geometric information: the cross-section centroid locations, self-weight distributions, and dimensions. Finally, the yellow section (on the right) of the workflow visualizes the applied loads and contains the core Python script that joins all inputs and executes the limit-analysis optimization. The tool then outputs the collapse-load multiplier and furnishes the predicted collapse mechanism, including the location of the internal horizontal hinge. Users can adjust input parameters in real-time, with immediate

feedback, allowing for rapid evaluation of how changes in geometry, material properties, or loading conditions impact the risk of collapse.

5 Results and Validation

The method previously presented is validated through the study of the eight benchmark collapse mechanisms, along with the related collapse multipliers, referred to a generalized wall, where the presence of openings is neglected. The thickness, height, and specific weight of the masonry wall will be kept constant and equal to respectively 0.4 m, 3 m for each level and 18 kg/m^3 . The graphs showing the results obtained from the visual scripting tool are given next in terms of collapse multiplier α versus the peculiar actions of each benchmark collapse mechanism.

The first example analyzed is the simple overturning mechanism involving a single level of the structure. In this case, the thickness was reduced from 0.4 m to 0.2 m for the analysis. As shown in Fig. 4(a), values of the collapse multiplier α were obtained by varying T , representing the presence of a tie rod, and P_s , the weight of the floor/roof acting on the wall, within the range from 0 to 10 kN and from 0 to 20 kN, respectively. It can be observed that T has a stabilizing effect as P_s increases. The presence of the tie rod, when combined with an increase in the floor weight, allows the α value to increase. In the absence of P_s , and with only T , this value would have more consistently increased. Moving on to the second benchmark case in Fig. 4(b) of multi-story simple overturning in the façade, the input parameters T and P_s are also considered variable. The trend is similar to the previous case, with the key difference being that the maximum value of the collapse multiplier is reduced by half. This is due to the increased slenderness of the macro-element, as it concerns a two-story façade. In the third case, shown in Fig. 4(c), involving a composed overturning mechanism, the varying parameters are still T and P_s . The trend closely follows that of the previous case, with higher values of the collapse multiplier due to the presence of the sidewall. The sidewall, being involved in the overturning mechanism, counteracts the collapse with its own weight. The fourth case in Fig. 4(d) involves the entire height of the wall, with the sidewalls participating in the overturning mechanism. In this scenario, in addition to T , the action exerted by a vault on the top level, F_v , varies. As shown by comparing the trend of the graph with that in Fig. 4(b) although the sidewall is involved and counteracts the overturning with its own weight, the collapse multiplier is much lower. This highlights how the presence of the vault is a determining and critical factor in triggering the mechanism, thus affecting the vulnerability of the structure. In this case as well, T helps increase the collapse multiplier. Figure 4(e) shows the trend of the collapse multiplier for the corner overturning case. In this case, once again the parameters T and P_s were varied, resulting in a graph trend consistent with the other overturning cases.

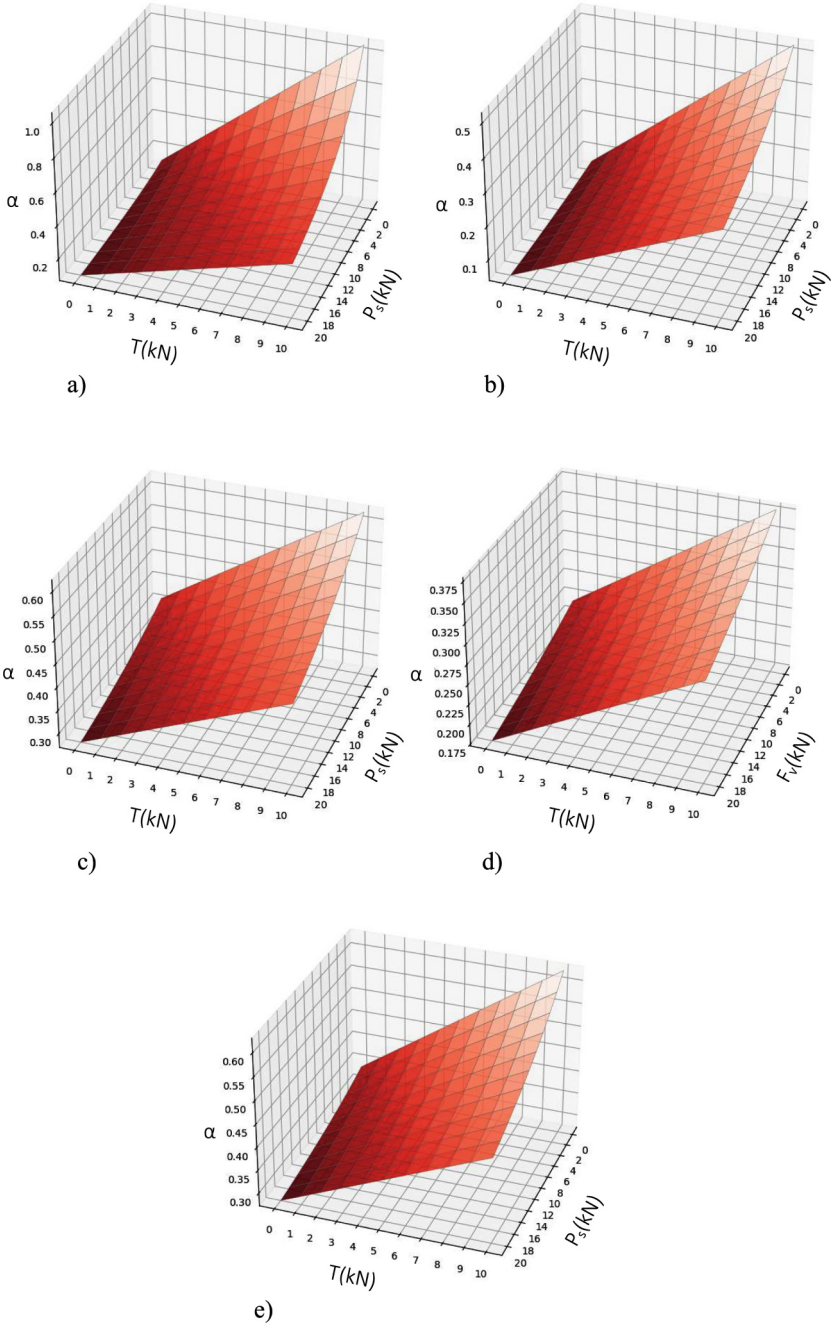


Fig. 4. Collapse multiplier versus the peculiar actions of each benchmark mechanism: the overturning mechanisms: a) simple overturning of a single-story wall, (b) simple overturning of a multi-story wall, (c) composed overturning of a single-story wall, (d) composed overturning of a multi-story wall, (e) composed overturning of a corner wall.

Figure 5 analyzes cases involving vertical or horizontal bending. In the first case, vertical bending (Fig. 5(a)) is considered for a single story, with F_v and N as varying parameters. The trend differs significantly from the overturning cases, with the mechanism being highly sensitive to changes in the values F_v and N . In this case, N plays a stabilizing role against F_v , ensuring a significant increase in the collapse multiplier.

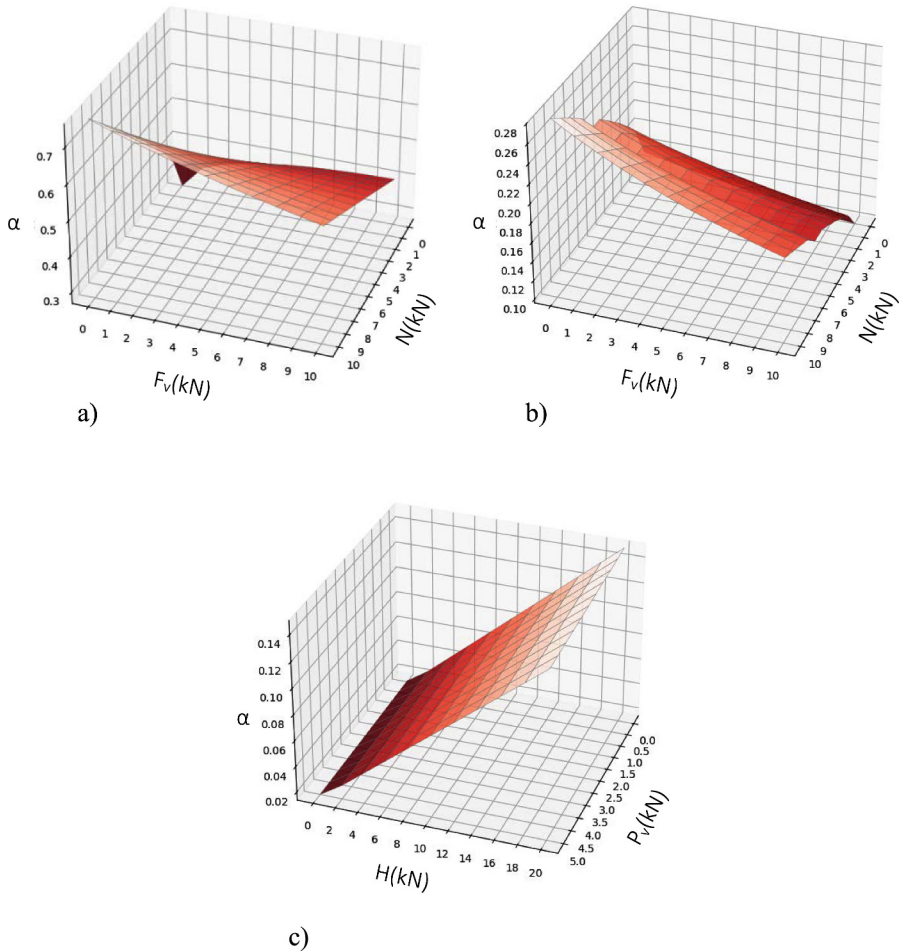


Fig. 5. Collapse multiplier versus the peculiar actions of each benchmark mechanism: the bending mechanisms: (a) vertical bending of a single-story wall, (b) vertical bending of a multi-story wall, and (c) horizontal bending of a single-story wall.

Fig. 5(b) represents the same mechanism for multiple stories. Here, the collapse multiplier is reduced, highlighting the structure's increased vulnerability compared to the single-story case, as the bending mechanism is more likely to develop along the entire height of the wall rather than being confined to a single level.

The last Fig. 5(c) shows the collapse mechanism due to horizontal bending, with H and P_v varying as the reaction force and vertical load, respectively. As observed, the presence of H increases the multiplier significantly, confirming its stabilizing effect in preventing the activation of the collapse mechanism.

6 Concluding Remarks

A visual scripting environment for kinematic limit analysis of masonry walls subjected to out-of-plane collapse mechanisms has been developed. The walls are modeled using a rigid-block-based approach, with limit analysis applied in its standard kinematic form to predict collapse mechanisms and related load multipliers through an optimization process.

A sensitivity analysis of the computed collapse load multiplier to different values of the live loads acting on eight benchmark out-of-plane mechanisms examined on a generalized (simplified) wall of fixed geometry, material and boundary conditions, has been carried out. The obtained results seem to prove the effectiveness of the proposed visual-scripting-based limit analysis tool.

The promoted user-friendly interactive approach allows quick identification of key factors, such as geometry, material properties, and applied load intensity, that influence the activation or prevention of collapse mechanisms in cracked walls. The tool also enables real-time evaluation of how adjustments, corresponding to structural restoration interventions, can improve safety, especially in post-seismic scenarios.

The results presented have to be viewed as a first step toward developing an efficient predictive tool for masonry walls safety assessment, with an ongoing research focusing on more complex masonry structural systems, sliding rigid-block mechanisms, and refining the rigid-block modeling to better reflect real masonry behavior including also the analysis of in-plane collapse mechanisms.

References

- Baggio, C., Trovalusci, P.: Collapse behaviour of three-dimensional brick-block systems using non-linear programming. *Struct Eng Mech.* **10**(2), 181 (2000)
- Block, P.P.: Thrust Network Analysis: Exploring Three-Dimensional Equilibrium. Massachusetts Institute of Technology: Doctoral Dissertation (2009)
- Casapulla, C., Maione, A., Ceroni, F., Prota, A., Di Ludovico, M.: Limit analysis and design-oriented approach for out-of-plane loaded masonry walls strengthened by grouted anchors. *Eng Struct.* **285**, 115991 (2023)
- Cifani, G., Petrucci, G., Lazzaro, D., D’Alessandro, S., Cialone, G., Martinelli, A., et al.: Repertorio dei meccanismi di danno, delle tecniche di intervento e dei relativi costi negli edifici in muratura. ITC-CNR (2006)
- D’altri, A.M., Sarhosis, V., Milani, G., Rots, J., Cattari, S., Lagomarsino, S., ..., De Miranda, S.: Modeling strategies for the computational analysis of unreinforced masonry structures: review and classification. *Archives of computational methods in engineering* (2020)
- Ferris, M.C., Tin-Loi, F.: Limit analysis of frictional block assemblies as a mathematical program with complementarity constraints. *Int J Mech Sci.* **43**(1), 209–224 (2001)

- Funari, M.F., Mehrotra, A., Lourenço, P.B.: A tool for the rapid seismic assessment of historic masonry structures based on limit analysis optimisation and rocking dynamics. *Appl Sci.* **11**(3), 942 (2021)
- Galassi, S., Zampieri, P.: A new automatic procedure for nonlinear analysis of masonry arches subjected to large support movements. *Eng Struct.* **276**, 115359 (2023)
- Gilbert, M.: Limit analysis applied to masonry arch bridges: state-of-the-art and recent developments. ARCH'07 – 5th International arch bridges conference (2007)
- Gilbert, M., Casapulla, C., Ahmed, H.: Limit analysis of masonry block structures with non-associative frictional joints using linear programming. *Comput Struct.* **84**(13–14), 873–887 (2006)
- Giuffrè, A.: A mechanical model for statics and dynamics of historical masonry buildings. In: *Protection of the Architectural Heritage Against Earthquakes*, pp. 71–152. Springer (1996)
- Heyman, J.: The stone skeleton. *Int J Solids Struct*, 249–279 (1966)
- Kumar, N., Barbato, M., Rengifo-López, E.L., Matta, F.: Capabilities and limitations of existing finite element simplified micro-modeling techniques for unreinforced masonry. *Res. Eng. Struct. Mater.* **8**(3), 463–490 (2022)
- Mazzeo, M., Laudani, R., Santoro, R.: Uncertainty effect on seismic capacity assessment in the out-of-plane failure mechanisms of masonry structures by probabilistic and non-probabilistic approaches. *Dev Built Environ.* **17**, 100366 (2024)
- Milano, L., Mannella, A., Morisi, C., Martinelli, A.: Illustrative sheets of the main local collapse mechanisms in buildings existing masonry and related kinematic models of analysis. Annex to the Repair and Strengthening Guidelines of structural elements, infills and partitions (2009)
- MIT. Ministero delle Infrastrutture e dei Trasporti. CNTC19 – Circolare applicativa delle Norme Tecniche delle Costruzioni di cui al D.M. 17-01-2018 (NTC 2018). *Gazzetta Ufficiale* N. 42 del 20-02-2018. 2019 (in Italian) (2019)
- Mousavian, E., Argiento, L. U., Casapulla, C.: Visual programming for macro-block analysis of multi-storey masonry buildings. 8th International Conference on Computational Methods in Structural Dynamics and Earthquake Engineering, COMPDYN 2021 (2021)
- Nodargi, N.A., Intrigila, C., Bisegna, P.: A variational-based fixed-point algorithm for the limit analysis of dry-masonry block structures with non-associative Coulomb friction. *Int J Mech Sci.* **161**, 105078 (2019)
- Portioli, F.P., Lourenço, P.B.: Nonlinear static analysis of masonry structures with mortar joints and cracking units by optimization-based rigid block models. *Earthq Eng Struct Dyn.* **53**(13), 3963–3982 (2024)
- Rippmann, M., Lachauer, L., Block, P.: Interactive vault design. *Int J Space Struct.* **27**(4), 219–230 (2012)
- Stockdale, G., Milani, G.: Diagram based assessment strategy for first-order analysis of masonry arches. *J Build Eng.* **22**, 122–129 (2019)
- Szabó, S., Funari, M.F., Lourenço, P.B.: Masonry patterns' influence on the damage assessment of URM walls: current and future trends. *Dev Built Environ.* **13**, 100119 (2023)

Open Access This chapter is licensed under the terms of the Creative Commons Attribution-NonCommercial-NoDerivatives 4.0 International License (<http://creativecommons.org/licenses/by-nc-nd/4.0/>), which permits any noncommercial use, sharing, distribution and reproduction in any medium or format, as long as you give appropriate credit to the original author(s) and the source, provide a link to the Creative Commons license and indicate if you modified the licensed material. You do not have permission under this license to share adapted material derived from this chapter or parts of it.

The images or other third party material in this chapter are included in the chapter's Creative Commons license, unless indicated otherwise in a credit line to the material. If material is not included in the chapter's Creative Commons license and your intended use is not permitted by statutory regulation or exceeds the permitted use, you will need to obtain permission directly from the copyright holder.

